

Distributed Out-of-core NMF of Dense and Sparse Data on CPU/GPU Architectures with Automatic Model Selection for Exascale Data

Ismael Boureima, Manish Bhattarai, Maksim Eren, Erik Skau, Philip Romero, Stephan Eidenbenz, and Boian Alexandrov,

Abstract—The need for efficient and scalable big-data analytics methods is more essential than ever due to the exploding size and complexity of globally emerging datasets. Nonnegative Matrix Factorization (NMF) is a well-known explainable unsupervised learning method for dimensionality reduction, latent feature extraction, blind source separation, data mining, and machine learning. In this paper, we introduce a new distributed out-of-core NMF method, named *pyDNMF-GPU*, designed for modern heterogeneous CPU/GPU architectures that is capable of factoring exascale-sized dense and sparse matrices. Our method reduces the latency associated with local data transfer between the GPU and host using *CUDA streams*, and reduces the latency associated with collective communications (both intra-node and inter-node) via *NCCL primitives*. In addition, sparse and dense matrix multiplications are significantly accelerated with GPU cores, resulting in good scalability. We set new benchmarks for the size of the data being analyzed: in experiments, we measure up to 76x improvement on a single GPU over running on a single 18 core CPU and we show good weak scaling on up to 4096 multi-GPU cluster nodes with approximately 25,000 GPUs, when decomposing a dense 340 Terabyte-size matrix and a 11 Exabyte-size sparse matrix of density 10^{-6} . Finally, we integrate our method with an automatic model selection method. With this integration, we introduce a new tool that is capable of analyzing, compressing, and discovering explainable latent structures in extremely large sparse and dense data.

Index Terms—NMF, Out-of-core, latent features, model selection, distributed processing, parallel programming, big data, heterogeneous computing, GPU, CUDA, NCCL, cupy



1 INTRODUCTION

Big data analysis plays a crucial role in many problems including human health, cyber security, economic stability, emergency response, and scientific discovery. With the increased accessibility to data and technology, datasets continue to grow in size and complexity. At the same time, the operational value of the information hidden in patterns in such datasets continues to grow in significance. Extracting explainable hidden features from large datasets, collected experimentally or computer generated, is important because the data presumably carry essential (but often previously unknown) information about the causality, relationships, and mechanisms of the investigated phenomenon. Discovering meaningful hidden patterns from data is not a trivial task because the datasets are formed only by directly observable quantities while the underlying processes or features, in general, remain unobserved, latent or hidden [15]. Non-negative Matrix Factorization (NMF) is a popular unsupervised learning method that extracts sparse and explainable latent features [22], that is often used to reveal explainable low-dimensional hidden structures

that represent and classify the elements of the whole dataset [13].

Analysis of vast amounts of (usually sparse) data via NMF requires novel distributed approaches for reducing computational complexity, speeding up the computation, and dealing with data storage and data movement challenges. The bulk of the NMF computations are matrix-matrix multiplications, which can be sped up by GPU accelerators. Although several parallel and distributed frameworks have been proposed to address this problem, the majority of them are constrained by their algorithmic designs, which limit their scalability for large-scale data (see details in Related work section). Many of the proposed algorithms result in high communication costs for data movement across different components of modern heterogeneous hardware platforms, such that data movement delays actually exceeds the actual computational cost. Our main contribution is a novel NMF parallel framework, called *pyDNMF-GPU*, that minimizes the data movement on GPUs, which in turn improves overall running times.

The main contribution and novelty of our work is the proposal of a new implementation of NMF with low memory complexity that enables the out-of-core factorization of very large datasets. Our proposed implementation, *pyDNMF-GPU*, takes advantage of the following three modern design choices: first, *pyDNMF-GPU* reduces the latency associated with local data transfer between the GPU and host (and vice-versa) by using *CUDA streams*; second, latency associated with collective communications (both intra-

- *Ismael Boureima, Manish Bhattarai, Maksim Eren and Boian Alexandrov are with the Theoretical Division, Los Alamos National Laboratory, Los Alamos, NM, 87544.*
- *Erik Skau, Philip Romero and Stephan Eidenbenz are with Computer, Computational, and Statistical Science Division, Los Alamos National Laboratory, Los Alamos, NM, 87544.*

Manuscript received December 1, 2021;

node and inter-node) is reduced by using *NCCL primitives*; third, we incorporate a batching approach for inter-node communication, which provides a unique ability to perform out-of-core NMF while using multiple GPUs for the bulk of computations. Enabling out-of-core factorization is very important because it removes the matrix size constraint imposed by the GPU memory, thus enabling analysis of datasets up to the cumulative size of all memory on the cluster. This is particularly required in order to address the challenges presented by the need to factorize the ever growing datasets. We utilize this unique ability of pyDNMF-GPU to demonstrate the decomposition of record large dense and sparse datasets.

In order to illustrate how *pyDNMF-GPU* can be used as a building block for more comprehensive workflows, we integrate *pyDNMF-GPU* with a model selection algorithm *pyDNMFk*⁰ that enables automatic determination of the (usually unknown) number of latent features on a large scale [4], [1], [12], [11]. The integrated model selection algorithm was used previously to decompose the worlds’ largest collection of human cancer genomes [3], defining cancer mutational signatures [2], as well as successfully applied to solve real-world problems in various fields.

This integration results in our out-of-core scalable tool, *pyDNMFk-GPU*, capable of estimating the number of latent features in extra-large *sparse* (tens of EBs) and dense (hundreds of TBs) datasets that can operate across CPU-GPU hardware. To the best of our knowledge, our framework is the first to identify hidden features in such a large-scale dense and sparse datasets.

In experiments on large HPC clusters, we show *pyDNMF-GPU*’s potential: we measure up to 76x improvement on a single GPU over running on a single 18 core CPU and we show good weak scaling on up to 4096 multi-GPU cluster nodes with approximately 25,000 GPUs, when decomposing a dense 340 Terabyte-size matrix and a 11 Exabyte-size sparse matrix of density 10^{-6} .

The main contributions of the paper include:

- Introducing a novel distributed algorithm with out-of-core support for NMF, for sparse and dense matrices, operating across CPU-GPU hardware.
- Report the first NCCL communicator accelerated NMF decomposition tool in distributed GPUs.
- Demonstrate the scalability of the framework over a record-breaking 340 Terabytes (TB) dense and 11 Exabytes (EB) sparse synthetic datasets.

The remainder of the paper is organized as follows: Section 2 gives a brief summary of NMF, and the existing parallel NMF implementations. In Section 3, we give the detail of the design considerations and choices for a salable, parallel, and efficient algorithm in different configurations of the data size and available GPU VRAM as well as the complexity of the new implementation. The demonstration of the efficacy of *pyDNMF-GPU* with different benchmark results and the validation of benchmark results on a synthetic dataset with a predetermined number of latent features is shown in Section 4. We finally conclude with summaries and suggestions of possible future work directions in Section 5.

0. *pyDNMFk*: <https://github.com/lanl/pyDNMFk>

2 BACKGROUND AND RELATED WORK

2.1 Non-negative matrix factorization algorithms

NMF [22] approximates the non-negative observational matrix $\mathbf{A} \in \mathbb{R}_+^{m \times n}$ with a product of two nonnegative factor matrices $\mathbf{W} \in \mathbb{R}_+^{m \times k}$ and $\mathbf{H} \in \mathbb{R}_+^{k \times n}$ where the columns of \mathbf{W} represent the latent features, while the columns of \mathbf{H} are the coordinates/weights of the analyzed samples (the columns of \mathbf{A}) in the reduced latent space, and k is the latent dimension of the data. The NMF minimization is based on alternating update of each one of these two factor matrices until convergence indicated by the condition $\|\mathbf{A} - \mathbf{WH}\|_F \leq \eta$ is reached. Here $\|\cdot\|_F$ is the Frobenius norm, $\|\mathbf{A}\|_F = \sqrt{\sum_i \sum_j a_{ij}^2}$, where a_{ij} is the element on row i and column j , and η is the desired tolerance. Each iteration consists of a \mathbf{W} -update sub-step followed by a \mathbf{H} -update sub-step, given by

$$\begin{aligned} \mathbf{W} &\leftarrow \arg \min_{\mathbf{W} \geq 0} \|\mathbf{A} - \mathbf{WH}\|_F^2, \\ \mathbf{H} &\leftarrow \arg \min_{\mathbf{H} \geq 0} \|\mathbf{A} - \mathbf{WH}\|_F^2, \end{aligned} \quad (1)$$

Algorithm 1 NMF(A, k, η, i_{max}) – Generic NMF

```

Set  $\mathbf{W} = random(m, k)$ ,  $\mathbf{H} = random(k, n)$ 
Set  $i = 0$ 
Set  $\eta_i = \eta + 1$  ▷ Ensure  $\eta_i > \eta$  to enter loop
while ( $\eta_i \geq \eta$  or  $i \leq i_{max}$ ) do
     $\mathbf{W} \leftarrow \mathbf{W} * \frac{(\mathbf{A} \otimes \mathbf{H}^T)}{\mathbf{W} \otimes \mathbf{H} \otimes \mathbf{H} + \epsilon}$  ▷  $\mathbf{W}$  update
     $\mathbf{H} \leftarrow \mathbf{H} * \frac{(\mathbf{W}^T \otimes \mathbf{A})}{\mathbf{W}^T \otimes \mathbf{W} \otimes \mathbf{H} + \epsilon}$  ▷  $\mathbf{H}$  update
     $\eta_i = \|\mathbf{A} - \mathbf{WH}\|_F$ 
     $i = i + 1$ ;
end while

```

The Frobenius norm (FRO) based multiplicative update(MU) algorithm is presented in Algorithm 1. In addition to the presented Frobenius norm-based MU algorithm (which leads to a Gaussian model of the noise [17]) other similarities (e.g., KL-divergence that corresponds to a Poisson model) can also be used in the NMF minimization. Also, based on the update rules, several variants of NMF algorithms exist such as Hierarchical Alternating Least Squares (HALS) [26], Alternating Non-negative Least Squares with Block Principle Pivoting (ANLS-BPP) [20], and Block coordinate descent algorithm (BCD) [19]. These algorithms have different advantages in the context of convergence rate, computational, and memory requirements. MU-based updates are computationally and memory-wise cheap at the cost of slower convergence. Whereas HALS, BCD, and ANLS-BPP have faster convergence rates at the cost of higher computational and memory requirements and high communication cost for parallel implementations. In our experiments we use FRO-based MU algorithm to demonstrate a record scalability on large dataset due to its lower computation and communication cost, which can easily be modified with another update algorithm or similarity metric.

TABLE 1: A comparison chart for different GPU based NMF implementations.

| Framework | GPU | Multi-GPU | Sparse | Out of Core | Remarks |
|--------------------------|-----|-----------|--------|-------------|--|
| <i>nmf-cuda</i> [9] | ✓ | ✓ | ✓ | ✓ | Multithreading support only |
| <i>NMF-mGPU</i> [24] | ✓ | ✓ | ✓ | ✓ | Communication inefficient design, entire factor need to be stored for each GPUs. |
| <i>mgs-mr</i> [21] | ✓ | ✓ | ✓ | ✓ | No distributed support. |
| <i>python-NMF</i> | ✓ | ✓ | ✓ | ✓ | No distributed support. |
| <i>NMF-spar</i> [30] | ✓ | ✓ | ✓ | ✓ | Inefficient scaling results. |
| <i>ALO-NMF</i> [25] | ✓ | ✓ | ✓ | ✓ | Shared memory implementation of optimized HALS algorithm & lack of distributed support |
| <i>PLANC</i> [18] | ✓ | ✓ | ✓ | ✓ | Not a significant gain of GPUs over CPUs and lack of ability to handle large sparse and dense data on GPUs. |
| <i>genten</i> [27] | ✓ | ✓ | ✓ | ✓ | Shared memory support only, runs on KOKKOS ⁸ backend, and no distributed memory support. |
| <i>pyDNMF-GPU (ours)</i> | ✓ | ✓ | ✓ | ✓ | NCCL based efficient implementation with significant speedup of GPUs over CPUs and demonstrated scaling performance over 340TB dense and 11EB sparse data. |

2.2 Related work on distributed NMF

To address the computational need of NMF for large datasets which involves multiple and repeated matrix-matrix multiplications of several orders in magnitude, several parallel implementations have been proposed. The existing parallel implementations can be grouped under two categories (i) with shared memory and (ii) with distributed memory. Majority of existing parallel works utilize shared-memory multiprocessor [9], [16], [25], [27] and shared memory GPUs [24], [25], [23], [27] via OpenMP and CUDA libraries respectively. A majority of distributed memory implementations rely on *MPI primitives* for distributed CPU [10], [18] and CUDA-aware *MPI primitives* for distributed GPU [18], [24] parallelization. Although shared-memory implementations drastically minimize the communication costs incurred for distributed memory implementation [25], there is a constraint on the amount of the data that can be decomposed by such frameworks. Due to this constraint, shared-memory implementation is often unable to provide computational/memory requirements needed for the current large-scale datasets.

Almost all distributed GPU implementations including *NMF-mGPU* [24] and *PLANC* [14] rely on significant data communication for the update of the factors. This involves either usage of CUDA-aware MPI primitives for data communication or MPI distributed memory offload through NVBLAS [14] without any multi-node GPU communicators. Such implementation leads to significant costs of data movement due to data on-loading/off-loading to/from the device which significantly raises communication cost compared to the computation cost for large data decomposition. This is previously illustrated with distributed BPP in *PLANC* [18], and distributed MU and BCD [10] where the communication cost is minimized by communicating only with the two-factor matrices and other partitioned matrices among MPI processes. These works attempt to reduce the bandwidth and data latency while using MPI collective communication operations. For distributed CPU implementations, this approach works well as communication cost is significantly lower compared to the computation cost. However, for GPU implementation, communication cost is higher due to device/host data transfer; therefore, communication cost is a limiting factor for the parallel performance when using a large number of GPUs.

8. KOKKOS: <https://github.com/kokkos/kokkos>

Table 1 illustrates the comparison against the existing parallel NMF implementations. Further, support for factorization of sparse datasets equally adds value for our new *pyDNMF-GPU* framework. Since many of the extra-large datasets, such as, the text corpora, knowledge graph embeddings (and, in general, most of the relational datasets), cyber network activity datasets, and many others, are highly sparse, having sparse decomposition support dramatically reduces the memory and computational requirements which otherwise would be a major bottleneck for the dense implementation. Despite the support for a sparse dataset for shared-memory in *ALO-NMF* and *genten* [25], [27] and for distributed memory in *PLANC* [18], there is no specific solution aiming to address the bottlenecks due to extracted dense factors and their communications for large sparse datasets. Even though the largest sparse sparsity, decomposing such datasets would be challenging for most of the existing frameworks. Even for such a small non-zero valued size, the corresponding dense factors could easily explode and also require an expensive communication of dense intermediate terms. However, our batching framework provides a solution by accommodating larger intermediate dense factors, which has not been addressed previously.

2.3 Rationale for *pyDNMF-GPU*

An unaddressed bottleneck for parallel NMF implementation is the decomposition of the data which would otherwise not fit in device memory. Out-of-core (or *online*) approach is a solution for this problem where the data is processed by the device in batches (block-based) to maximize the computational efficiency and overcome the memory bottleneck. Currently, out-of-core implementations only exist for SVD decomposition [31], [28]. To this end, our out-of-core implementation of NMF on distributed GPU platforms is a novel contribution. In addition, integrating such capability with distributed memory adds more value to the proposed framework.

NCCL is a set of powerful collective communication primitives for GPU which has already demonstrated accelerated performance for deep learning applications [29], [5], [7], [6], [8]. However, the utilization of NCCL for NMF has been unexplored so far. This provides us the opportunity to demonstrate its superior scaling performance over every other existing framework. In this work, we introduce a novel NCCL based distributed NMF with a state-of-the-art efficient scaling performance across multiple nodes for an online factorization of record size large scale data. This multiplicative update algorithm is also designed to minimize the communication cost and maximize the bandwidth to achieve peak performance of the GPU hardware.

3 *pyDNMF-GPU* FOR HETEROGENEOUS SYSTEMS

3.1 Distributed implementation

An efficient implementation of NMF for distributed heterogeneous systems should avoid high costs associated with communication (data transfer) resulting from poor consideration for data locality in the distribution of the

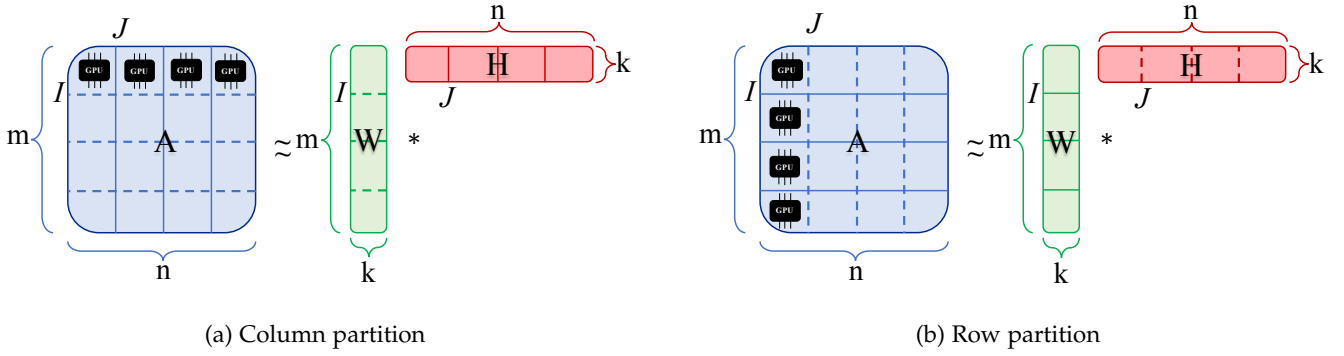


Fig. 1: Illustration of distributed matrix A and co-factors W and H in $CNMF$ and $RNMF$ distributed partitions respectively in (a) and (b). Solid lines show distributed partition boundaries, and dashed lines show local partition segmentation in batch for out of core decomposition.

computational work. Furthermore, cases with limited resources such as available combined GPUs memory, will require additional considerations and various trade-offs. For instance, it is sometimes better to replicate data over the distributed grid in order to reduce communication, and other times, it is acceptable to use batching techniques, which can increase communication cost, in order to lower the memory complexity.

Our implementation considers two data partition strategies based on the shape of $m \times n$ matrix A ; a column (vertical) partition, $CNMF$ employed when $n > m$, and a row (horizontal) partition, $RNMF$, used otherwise.

Algorithm 2 $H_{Update} - H$ Update in $CNMF$

```

Set  $I = m/n_B$  ▷ Batch size
Set  $J = n/N$  ▷ Partition size
Set  $j_0 = gID * J, j_1 = (gID + 1) * J$ 
Set  $WTA = zeros(k, J)$ 
Set  $WTW = zeros(k, k)$ 
Set  $H = zeros(k, J)$ 
for  $p$  in 0 to  $n_B$  do
  Set  $i_0 = p * I, i_1 = (p + 1) * I$ 
   $A_p \leftarrow copyH2D(A[i_0 : i_1, j_0 : j_1])$  ▷
   $W_p \leftarrow copyH2D(W[i_0 : i_1, :])$  ▷
   $WT \leftarrow transpose(W_p)$  ▷
   $WTA \leftarrow WTA + WT @ A_p$  ▷
   $WTW \leftarrow WTW + WT @ W_p$  ▷
end for
 $H \leftarrow (H * WTA) / (WTW @ H + \epsilon)$  ▷

```

Assuming a distributed system with N GPUs, where each GPU is indexed by its global rank gID . In the $CNMF$ approach illustrated in Fig. 1a, the j^{th} GPU with $gID = j$ will work on array partitions $A[:, j_0 : j_1]$, W and $H[:, j_0 : j_1]$, where $j_0 = j \times J, j_1 = (j+1) \times J$, and $J = n/N$ (partition size). Similarly, I is batch size where $I = m/n_B$ and for standard distributed version $n_B = 1$. This parameter is only effective for out of core implementations discussed

in the next section. For $CNMF$, each GPU gets a full copy of W (W is replicated) and a unique partition of A and H . This translates into a segmentation of arrays A and H on global memory illustrated with solid lines in Fig. 1a. These solid lines indicate boundaries in global memory, and consequently help conceptualize where the communication is required whenever information is exchanged from one bounded region to another. In $CNMF$, the H -update is embarrassingly parallel since $W^T W$, $(W^T W)H$, and $W^T A$ can all be computed locally on each GPU. W -update on the other hand is not fully parallel, as it will require two all-reduce-sum communications to compute AH^T and HH^T as indicated in alg. 2.

In the $RNMF$ approach illustrated in Fig. 1b, the i^{th} GPU with $gID = i$ will work on partitions $A[i_0 : i_1, :]$, $W[i_0 : i_1, :]$ and H , where $i_0 = i \times p, i_1 = (i + 1) \times J$ and $J = m/N$. Note that in this approach H is replicated on the different GPUs and A and W are distributed, as shown in Fig. 1b. In this approach, the W -update is embarrassingly parallel since HH^T , $W(HH^T)$, and AH^T can all be computed locally on each GPU. H -update on the other hand will require two all-reduce-sum communication to compute $W^T W$ and $W^T A$.

Communication takes place through various channels with different bandwidth and latency. We refer to communications between GPUs on the same node, as intra-node communications, and those between GPUs on different nodes as inter-node communications. The latter often have the lowest bandwidth and highest latency, and could easily become bottlenecks for distributed algorithms such as NMF. For these practical reasons, in our implementation, we avoid all-reduce collective calls, as much as possible. When $n > m$, $CNMF$ is more efficient than $RNMF$ because it costs less to communicate AH^T which is of size $m \times k$. Conversely, when $m > n$, $RNMF$ is more efficient, because it cost less to communicate $W^T A$ which is of size $k \times n$.

The total VRAM required to factorize A of size $size(A) = S_A$ (in Bytes) is typically in the order of $S_{NMF} \sim 3 \times S_A$. One fold of S_A to store A in memory, another fold to compute the intermediate product $W @ H$ when checking the convergence condition $\|A - WH\|_F \leq \eta$, and almost one more fold to store the co-factors W, H , and heavy intermediate products such as $W^T @ A$ or $A @ H^T$. When the total available combined GPU VRAM, S_{GV} , is

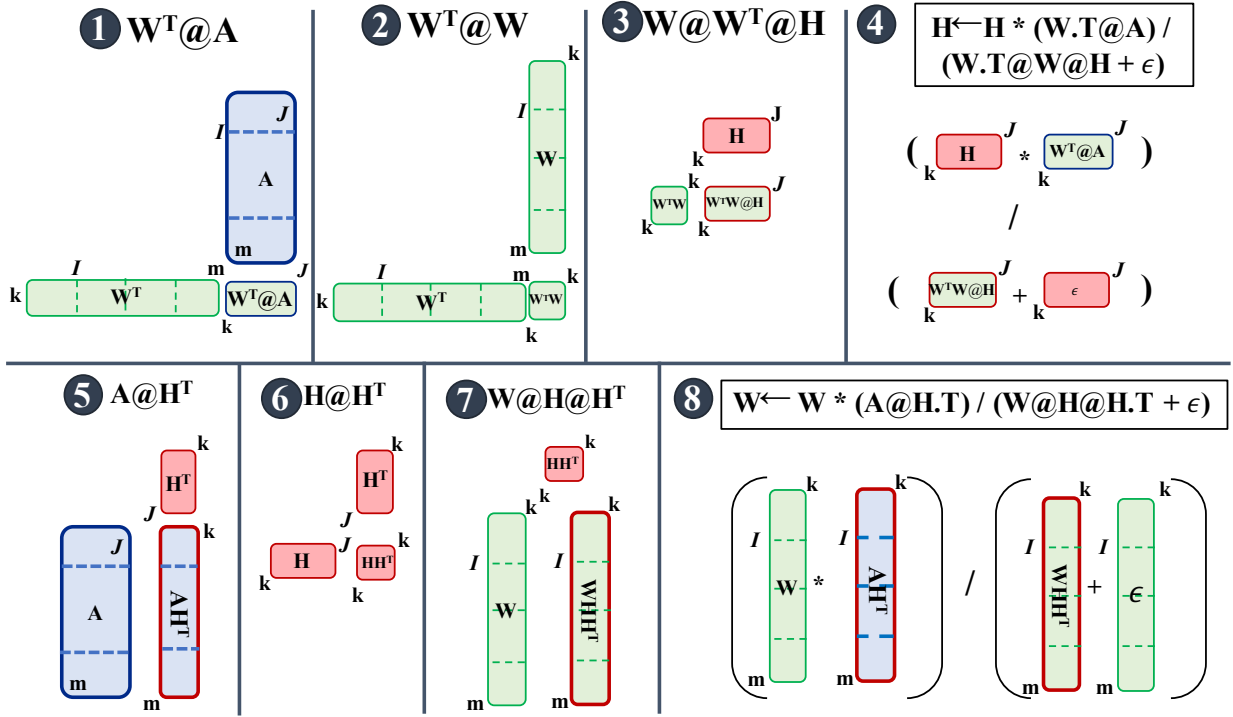


Fig. 2: Illustration of the batched multiplicative update algorithms 3 and 2 for the column partition (CNMF). Green array is duplicated across different MPI ranks. Blue and red arrays are distributed, and only red array is cached on device. For CNMF, I is out of core block size (batch size) and J is distributed block size.

Algorithm 3 $W_{\text{Update}} - W$ Update in $CNMF$

```

Set  $I = m/n_B$                                 ▷ Batch size
Set  $J = n/N$                                     ▷ Partition size
Set  $j_0, j_1 = gID * J, (gID + 1) * J$ 
 $HT \leftarrow \text{transpose}(H)$ 
 $HHT \leftarrow H @ HT$                           ▷  $[\mathcal{O}_c(k^2 * I), \mathcal{O}_m(k \times k)]$ 
 $HHT \leftarrow \text{All\_Reduce}(HHT)$ 
for  $p$  in 0 to  $n_B$  do
  Set  $i_0 = p * I, i_1 = (p + 1) * I$ 
   $A_p \leftarrow \text{copyH2D}(A[i_0 : i_1, j_0 : j_1])$ 
   $[ \mathcal{O}_c(1), \mathcal{O}_m(I \times J) ]$ 
   $W_p \leftarrow \text{copyH2D}(W[i_0 : i_1, :])$ 
   $[ \mathcal{O}_c(1), \mathcal{O}_m(I \times k) ]$ 
   $WHHT_p \leftarrow W_p @ HHT$ 
   $[ \mathcal{O}_c(k \times J \times I), \mathcal{O}_m(I \times k) ]$ 
   $AHT_p \leftarrow A_p @ HT$ 
   $[ \mathcal{O}_c(k^2 \times I), \mathcal{O}_m(I \times k) ]$ 
   $AHT_p \leftarrow \text{All\_Reduce}(AHT_p)$ 
   $W_p \leftarrow W_p * AHT_p / (WHHT_p + \epsilon)$ 
   $[ \mathcal{O}_c(k \times J), \mathcal{O}_m(I \times k) ]$ 
end for

```

lower than S_{NMf} , as it is the case in practical big data applications, batching techniques are imperative, and will in most cases increase intra-node and inter-node communication overheads. Although this can significantly affect the performance of the algorithm, proper use of CUDA streams can reduce performance loss, by overlapping compute and data transfers.

3.2 Out-of-core implementation

In out-of-core situations when $S_{GV} < S_{NMf}$, light arrays are cached on GPU memory, and heavier arrays are kept on host memory and batched to respective GPUs as needed. To illustrate, let I be a batch size control parameter. In $RNMf$ ($CNMF$) the number batches is then given by $n_B = m/I$ ($n_B = n/I$). In the extreme case where both m and n are very large, only the light array, $W[J, :]$ is cached on GPU memory, and heavier arrays $A[J, b_0 : b_i]$ ($A[b_0 : b_1, J]$) and $H[:, b_0 : b_1]$ ($W[b_0 : b_1, :]$) batched to their respective GPUs, such that for the b^{th} batch, $b_0 = b \times I$ and $b_1 = (b + 1) \times I$. The illustration in Figure 2 shows the different intermediate products in our implementation of the *batched CNMF* approach, where batch delimitation are represented with dashed lines. The top row shows all intermediate products computed during H -update, and products computed in W -update are shown in the bottom row. Intermediate products $W^T @ A$ and $W @ W^T$ can be computed with n_B independent batches each containing $[W^T @ A]_b$ and $[W^T @ W]_b$ sub-products. Each batch is queued to a non-default CUDA stream Stm_b along with the transfer of $A_b[b_0 : b_i, J]$ and $W_b[b_0 : b_i, :]$, and when calculated, each sub-product is added to a local accumulator. Special batch en-queuing and de-queuing policies are implemented with CUDA events, so as to limit (control) the number of concurrent batches on GPU to n_{cb} . This way, the memory requirement for H -update is bounded by $n_{bc} \times [I \times J]$, as $W^T W @ H$ and $H * (W^T A) / (W^T W H + \epsilon)$ have a $k \times J$ memory requirement. This is important especially when dealing with large sparse arrays which can be cheap to cache on device, but can also have co-factors becoming prohibitively expensive

to cache when k becomes large. For instance, in *CNMF*, when $m \sim 10$ million, the size of \mathbf{H} will approximate 20GB in single precision when $k \sim 512$.

Intermediate products $\mathbf{A}@\mathbf{H}^T$ and $\mathbf{W}@\mathbf{H}\mathbf{H}^T$ of the \mathbf{W} -update are computed similarly to $\mathbf{W}^T@\mathbf{A}$ and $\mathbf{W}@\mathbf{W}^T$, except $\mathbf{A}@\mathbf{H}^T$ will require an intermediate *all-reduce-sum* of sub-products $[\mathbf{A}@\mathbf{H}^T]_b$ of batches of same number from the different GPUs (see alg. 3).

Note that the use of batches here will only increase *intra-node* communication due to mem-copies, as it is not possible to cache \mathbf{A} and \mathbf{W} on device. Additional data transfer latency is reduced using low latency NVIDIA communication collectives library (NCCL) instead of MPI, for both intra-node and inter-node communications. Communication performance gain using NCCL over MPI is discussed in Section 4.1, and much more in details by Awan [7].

3.3 Complexity analysis

In this section, we analyse the upper bound limits of compute and memory complexities of the proposed NMF algorithms. Time complexity associated with compute is denoted with $\mathcal{O}_c()$, and the memory complexity is denoted with $\mathcal{O}_m()$. Both complexities are itemized in the form of comments, in the different NMF algorithms below. Algorithms for H_{update} and W_{update} in *CNMF* are respectively given in algorithms 2 and 3. While both have a similar compute complexity of $\mathcal{O}_c(k \times J \times I)$, and a memory complexity of $\mathcal{O}_m(I \times J)$, W_{update} is expected to have a longer execution time because of latency introduced by each all-reduce-sum $AR()$ call.

4 BENCHMARKS RESULTS AND DISCUSSION

4.1 Hardware infrastructure and software environment

Benchmark tests were performed on two different HPC clusters to illustrate the portability and scalability of *pyDNMF-GPU*. The larger cluster, Summit, peaks at over 200 petaflops in double-precision theoretical performance, and is composed of 4,600 IBM AC922 compute nodes, with two IBM POWER9 CPUs and six NVIDIA Volta V100 GPUs each. The POWER9 CPUs have 22 cores running at 3.07 GHz. The six NVIDIA Tesla V100 GPUs in each node provide a theoretical double-precision arithmetic capability of approximately 40 teraflops with VRAM memory of 16GB/GPU. Dual NVLink 2.0 connections between CPUs and GPUs provide a 25-GB/s transfer rate in each direction on each NVLink, yielding an aggregate bidirectional bandwidth of 100 GB/s. The nodes are networked in a non-blocking fat-tree topology by infiniband. Summit deploys a RHEL 7.4 OS and IBM Job step manager jsrun to run compute jobs. Jsrun provides a fine control of how node-level resources are allocated on these systems, including CPU cores, GPUs, and hardware threads. The smaller cluster, an in-house cluster, has 133 compute nodes with dual Xeon E5-2695 v4 CPUs and four NVIDIA Pascal P100 GPGPUs each. Each NVIDIA Pascal P100 GPGPU has 16GB VRAM and uses PCIE 16X gen 3 Links. The cluster peaks at 1850TF/s and uses an infiniband interconnect.

4.2 GPU vs CPU Scalability

The performance gained using GPU over CPU is assessed with speedup computed as the ratio of time measure on CPU with *pyDNMFk*[11], to time measure on GPU with *pyDNMF-GPU*. For this study we used a dense matrix of shape and size S_A of memory (in bytes) that respectively scale as $[N \times 65536, 32768]$ and $N \times 8GB$, where N is the number of GPU or CPU units. Speedup measured on the small cluster are reported in Fig 3. Speedup in NMF time as a function of number of units for various k are shown in Fig 3a. First we note an increasing speedup with increasing number of units, and second we note a decreasing performance with increasing k when $k \geq 32$. The low performance observed at $k < 32$ is explained by low GPU occupancy. The best performance is obtained when $k = 32$, peaking at 76X. We also report speedup in communication time as a function of number of units for various k in Fig 3b. We note $\sim 100X$ speedup when $N > 2$, the compute grid size above which inter-node communications start. This clearly demonstrates the advantage of using NCCL in *pyDNMF-GPU* over MPI in *pyDNMFk*.

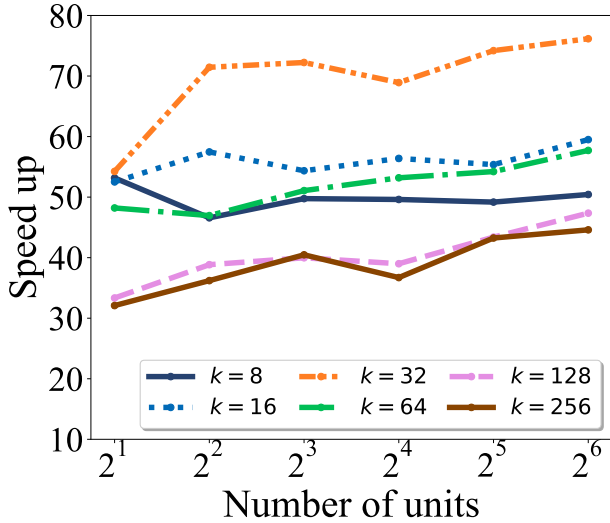
4.3 Strong and Weak Scalability

The scalability of the proposed NMFk algorithm is assessed using both strong and weak scaling analysis. This scaling study measures NMF execution time for a given problem size as a function of the number of compute units. Full compute nodes (with 4 GPUs each) are chosen as a compute unit in strong scaling analysis, while individual GPUs are chosen as compute units in weak scaling analysis. The problem size S_A is chosen so as to use most of the available 16GB VRAM per GPU. To this end, S_A is fixed at $S_A \approx 4 \times 8GB = 32GB$ in strong scaling analysis, and chosen to scale as $S_A \approx 8GB \times N$ in weak scaling analysis. This is accomplished by generating a random synthetic array A of shape $[4 \times 65536, 32768]$ and $[N \times 65536, 32768]$ respectively in both strong and weak scaling. Cases of sparse A with density 10^{-5} were also studied, and for those cases, A was generated as a random synthetic array of shape $[4 \times 2097152, 65536]$ in strong scaling analysis, and of shape $[N \times 2097152, 65536]$ was chosen in weak scaling analysis.

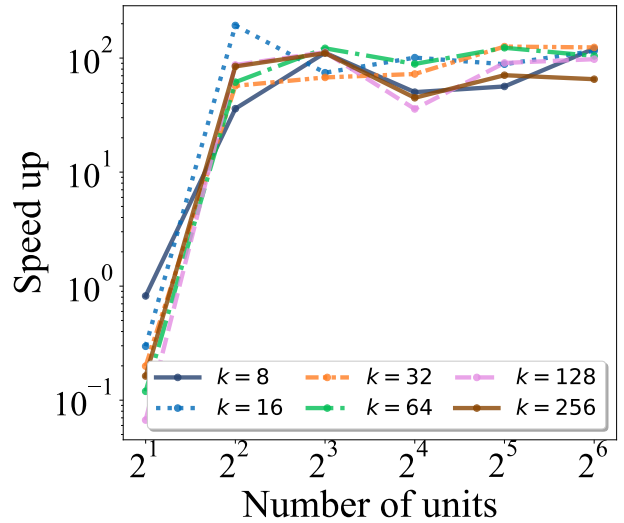
4.3.1 Strong scalability:

Strong scaling results for cases where $k = 8, 16, 32, 64, 128, 256$ are shown Fig. 4a. NMF time is found to increase with k , and to decrease with increasing number of compute nodes. Good strong scaling is indicated by a linear decrease of NMF time with increasing compute grid size, and such behaviour is only observed in select parts of the obtained results. Strong scaling is maintained up to a count of 8 nodes when $k = 8$, then to 4 nodes when $k = 16$, and lost when $k > 16$. Identical scaling is observed for cases where A is sparse, as shown in Fig. 4b.

The worst case scenarios, when $k = 256$, can be diagnosed from breakdown of H_{update} , W_{update} and combined all-reduce-sum (AR) execution time, as detailed in Fig. 4c. H_{update} is shown to maintain good scaling at all compute grid sizes, while W_{update} had a poor scaling at each tested compute grid size. W_{update} 's poor scaling is strongly influenced by AR communications time, which



(a) Speedups of the compute times for various latent dimensions on different numbers of compute units.



(b) Speedups of the communication times for various latent dimensions on different numbers of compute units.

Fig. 3: Results of benchmarking experiment showing speedup gain using N GPUs vs N CPUs, for various k . Speedup gained on NMF calculation time is shown in (3a) and speedup gained on communication time is shown in (3b). From (3a), a significant speedup is achieved on GPUs compared to corresponding CPUs count and (3b) significant speedup is achieved with the NCCL communicator on GPUs compared to MPI on CPUs.

already makes up more than 80% of W_{update} at 2 node count, and which increases non-linearly with node count. At full grid size, AR time makes up more than 98% of W_{update} , this in turn influences the overall NMF time dominated by W_{update} time. The same explanation applies to cases where A is sparse as one can interpret from Fig 4d.

4.3.2 Weak scalability:

Weak scaling results for cases with $k = 8, 16, 32, 64, 128, 256$ are shown Fig. 5a. Good weak scaling is indicated by constant NMF time with increasing number of compute units, and this is observed only when $N > 8$. The lack of scaling when $N < 8$ can be explained using the breakdown of H_{update} , W_{update} and combined AR execution time for the case where $k = 256$, shown in Fig. 5c. While W_{update} maintains a perfect weak scaling at all N , H_{update} is influenced by AR communications time which increases with GPU count. Communication grows with noticeable transitions indicating the use of slower channels. The first transition is from $N = 1$ to $N = 2$ indicating the beginning of *intra* – *node* communication between GPUs on the same node. While growing with N , *intra* – *node* communication remains a small portion of W_{update} ($\sim 10\%$). The next major transition occurs between $N = 4$ and $N = 8$, indicating the beginning of *inter* – *node* communication, which quickly saturates to $\sim 40\%$ of W_{update} by $N = 32$. Identical weak scaling is observed for cases where A is sparse, as shown by plots in Fig. 5b, and the explanation for lack of scaling when $N < 8$ is consistent with the explanation given above for the case where A is dense, as one can interpret from Fig. 5d.

While all scaling results were obtained with $CNMF$, similar results will be obtained with A^T using $RCNF$.

4.4 Sparse Scalability

Given our interest in exa-scale data, the proposed implementation was tested on a dense matrix of shape $[2618523648; 32768]$ with a size of $\sim 340TB$, and a sparse matrix of shape $[2.89 * 10^{12}, 1.05 * 10^6]$ with sparsity 10^{-6} and size of $\sim 11EB$ ($\sim 34TB$ when compressed in a sparse format). The compute grid consisted of 4096 nodes with 6 GPUs of 16 GB VRAM each, totaling to a combined 394TB VRAM. While that is not enough to efficiently factorize either of the two matrices, we chose to cache A and co-factors, and batch the compute of heavy intermediate products. This way, we are able to reduce performance loss by avoiding unnecessary data transfers from host to device, and vice-versa. Weak scaling results for the problem sizes of interest, factorized with the new batched approach, is shown in Figures 6a and 6b for dense and sparse data respectively. While results for sparse data indicate good weak scaling, performance on dense data was moderately affected by high communication latency.

4.5 Validation of model selection: *pyDNMFk-GPU*

To demonstrate the correctness of the *pyDNMFk-GPU* on big synthetic datasets, we determine the number of latent features on a synthetic terabyte size matrix (with a pre-determined number of features) and show that estimation is performed correctly. We generate a random matrix of dimensions 8388608×32768 as a product of two random matrices, W and H , with latent feature count of $k = 8$. We construct W with Gaussian features with different statistical means. The *pyDNMFk-GPU* silhouette analysis corresponding to this decomposition is shown in Fig. 7a and the correctness of features is shown with confusion matrix in Fig. 7b. *pyDNMFk-GPU* estimates $k = 8$ as the minimum Silhouette score is high and relative error is low.

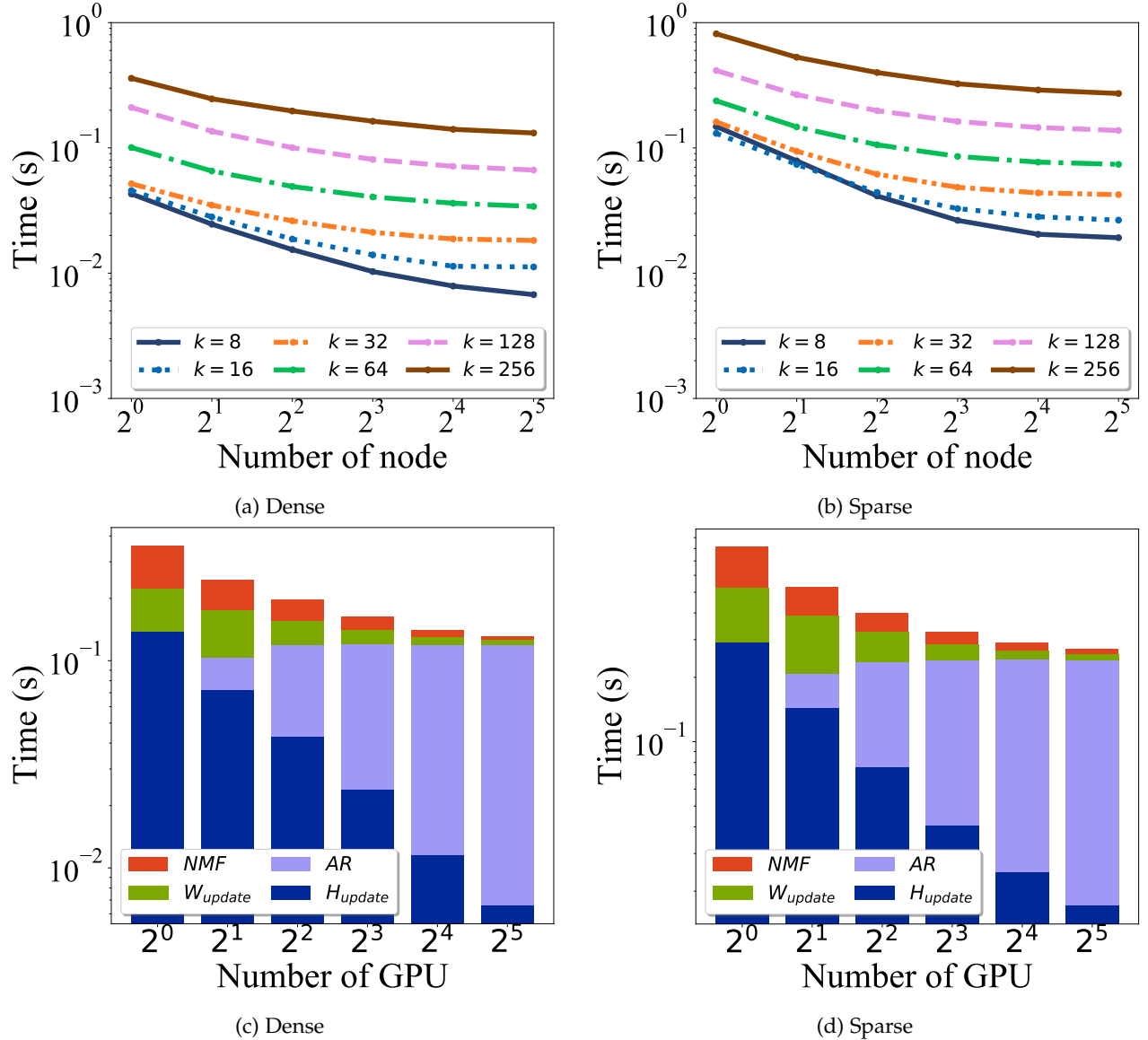


Fig. 4: Results of strong scaling study performed on smaller cluster. NMF time vs number of node for various k plotted in (4b) and (4a), respectively for dense and sparse A . For the case $k = 8$, execution time of H_{update} , W_{update} and All-reduce communication are compared in (4c) and (4d), respectively for dense and sparse A .

Differently, for $k > 8$, the minimum silhouette score drops suddenly as the solutions begin to fit the noise (Fig 7a). Fig 7b shows a Pearson correlation matrix which illustrates a large correlation between the features of ground truth $W_{Groundtruth}$ and the corresponding $pyDNMFk$ -GPU extracted $W_{Predicted}$ for $k = 8$. The analysis took approximately 1 hour on the smaller cluster to correctly estimate the latent features. The average reconstruction error for the data is $\sim 4\%$ with the Frobenius norm objective and MU update optimization. Our experiment demonstrates that $pyDNMFk$ -GPU correctly estimates the number of latent features in addition to its scalability for large datasets as discussed in previous sections.

5 CONCLUSION

In this paper we demonstrated a new scalable framework, $pyDNMFk$ -GPU, for non-negative matrix factorization based

on custom multiplicative updates, with automatic determination of the number of latent features on Exa-scale data. The framework is built for heterogeneous compute platforms, and is designed to optimize arithmetic intensity using NCCL to minimizing communication cost. Optimality was demonstrated via strong and weak scaling benchmarks, and speedup gains on GPU over CPU were found to vary with k and to increase with size of HPC system. Consistent with complexity analysis, inter-node communication was found to significantly affect strong scaling performance. The importance of our use of CUDA streams in batching techniques when VRAM is limited was discussed and demonstrated with factorizing a dense data set of size 340TB. We also presented a novel out-of-core NMF for single GPU and multi-GPU systems. Support for sparse data set has been shown, and was found to have good scaling on a heterogeneous system with up to 25,000 GPUs. For correctness, we performed the decomposition of a large synthetic data with

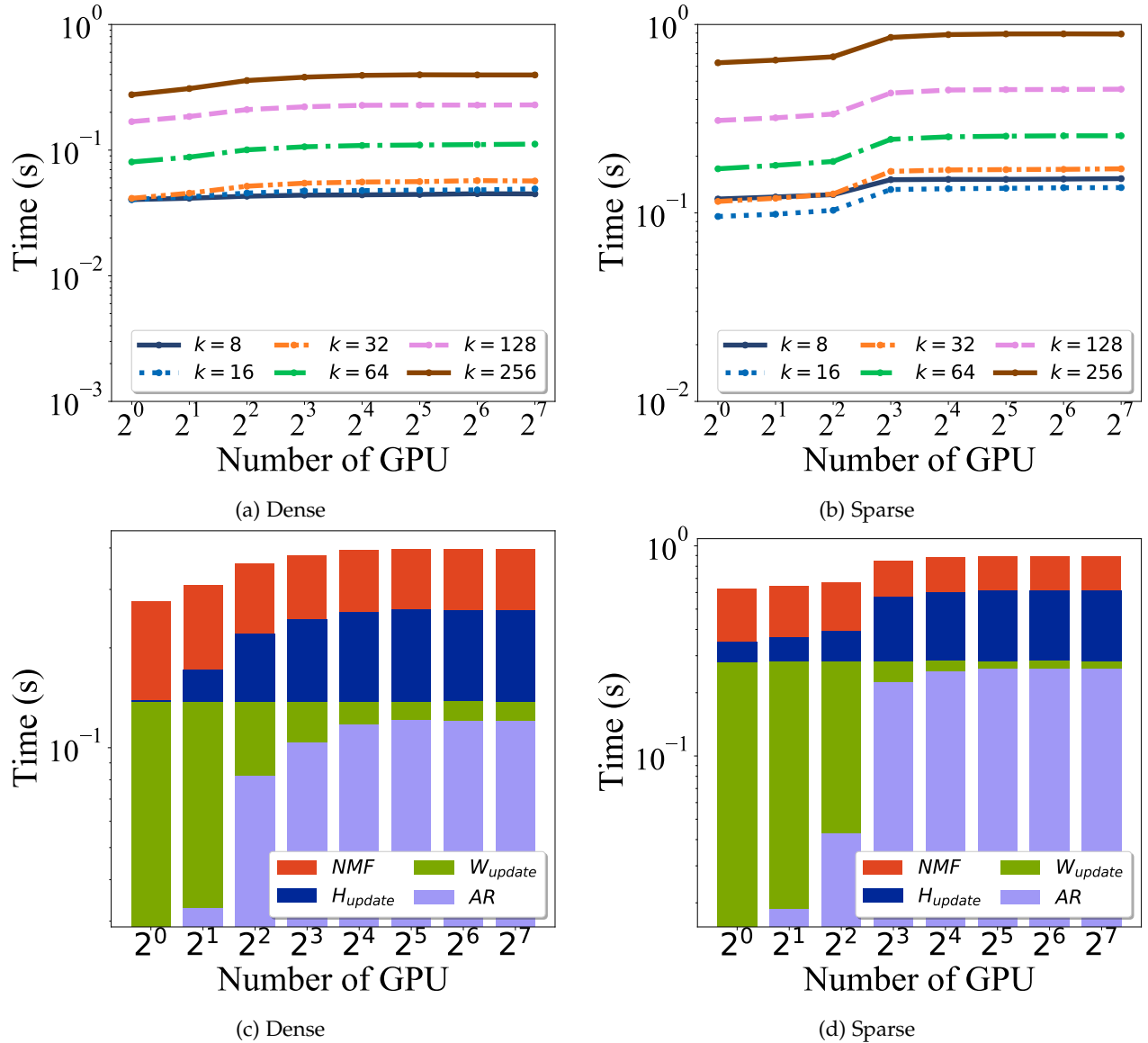


Fig. 5: Results of weak scaling study performed on a heterogeneous system with 4 Pascal P100 per compute nodes. NMF time vs number of GPU for various k are plotted in (5b) and (5a), respectively for dense and sparse A . For the case $k = 8$, execution time of H_{update} , W_{update} and All-reduce communication are compared in (5c) and (5d), respectively for dense and sparse A .

a predetermined number of latent features and factors and compared the estimated result with the ground truth.

ACKNOWLEDGMENT

This research was funded by DOE National Nuclear Security Administration (NNSA) - Office of Defense Nuclear Non-proliferation R&D (NA-22) and by U.S. Department of Energy National Nuclear Security Administration under Contract No. DE-AC52-06NA25396 through LANL laboratory directed research and development (LDRD) grant 20190020DR.

CONFLICT OF INTEREST

The authors declare that they have no conflict of interest.

REFERENCES

- [1] Alexandrov, B.S., Alexandrov, L.B., Iliev, F., Stanev, V.G., Vesselinov, V.: Source identification by non-negative matrix factorization combined with semi-supervised clustering (2020), uS Patent 10,776,718
- [2] Alexandrov, L.B., Kim, J., Haradhvala, N.J., Huang, M.N., Ng, A.W.T., Wu, Y., Boot, A., Covington, K.R., Gordenin, D.A., Bergstrom, E.N., et al.: The repertoire of mutational signatures in human cancer. *Nature* 578(7793), 94–101 (2020)
- [3] Alexandrov, L.B., Nik-Zainal, S., Wedge, D.C., Aparicio, S.A., Behjati, S., Biankin, A.V., Bignell, G.R., Bolli, N., Borg, A., Børresen-Dale, A.L., et al.: Signatures of mutational processes in human cancer. *Nature* 500(7463), 415 (2013)
- [4] Alexandrov, L.B., Nik-Zainal, S., Wedge, D.C., Campbell, P.J., Stratton, M.R.: Deciphering signatures of mutational processes operative in human cancer. *Cell reports* 3(1), 246–259 (2013)
- [5] Awan, A.A., Bédorf, J., Chu, C.H., Subramoni, H., Panda, D.K.: Scalable distributed dnn training using TensorFlow and CUDA-aware MPI: Characterization, designs, and performance evaluation. In: 2019 19th IEEE/ACM International Symposium on Clus-

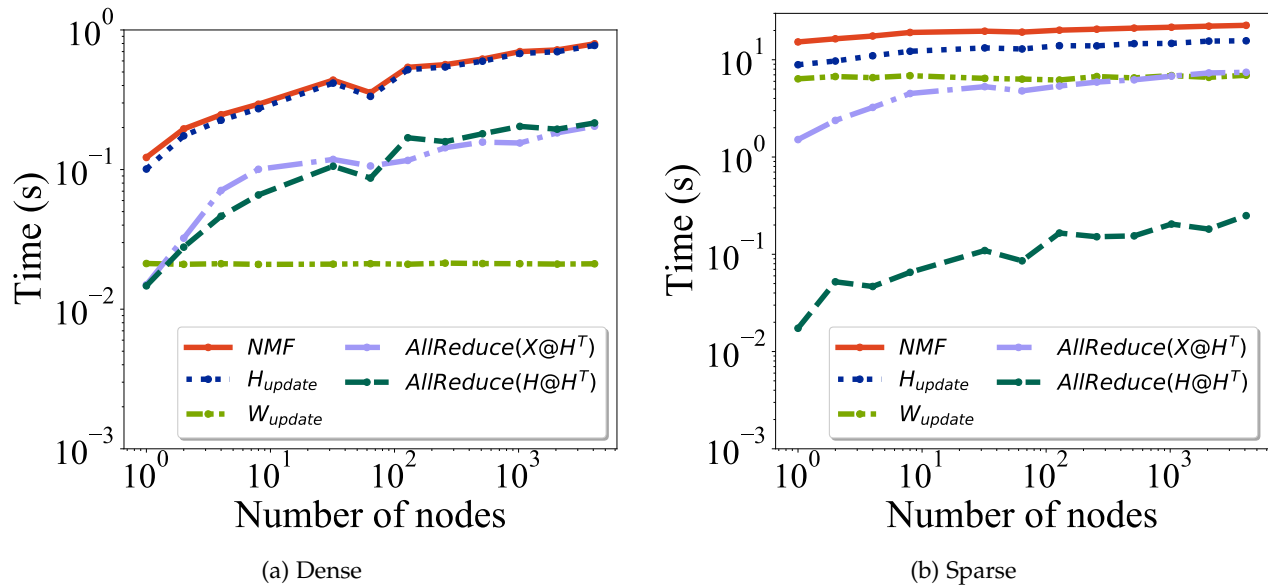


Fig. 6: Results of weak scaling study for dense and sparse A are shown respectively in (a) and (b). The study was performed on 4096 compute nodes with 6 GPUs per node.

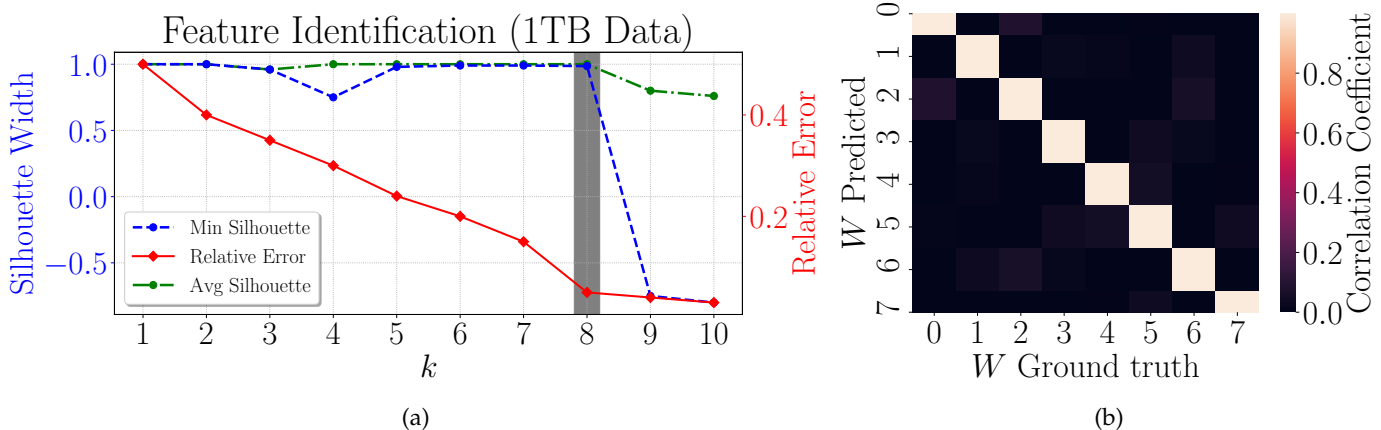


Fig. 7: (a) Estimation of number of hidden features($k=8$) through Silhouette analysis [12]. (b) Pearson correlation between columns of ground truth W and reconstructed W .

- ter, Cloud and Grid Computing (CCGRID). pp. 498–507. IEEE (2019)
- [6] Awan, A.A., Chu, C.H., Subramoni, H., Panda, D.K.: Optimized broadcast for deep learning workloads on dense-GPU InfiniBand clusters: MPI or NCCL? In: Proceedings of the 25th European MPI Users’ Group Meeting. pp. 1–9 (2018)
- [7] Awan, A.A., Hamidouche, K., Venkatesh, A., Panda, D.K.: Efficient large message broadcast using NCCL and CUDA-aware MPI for deep learning. In: Proceedings of the 23rd European MPI Users’ Group Meeting. pp. 15–22 (2016)
- [8] Awan, A.A., Manian, K.V., Chu, C.H., Subramoni, H., Panda, D.K.: Optimized large-message broadcast for deep learning workloads: MPI, MPI+ NCCL, or NCCL2? parallel computing **85**, 141–152 (2019)
- [9] Battenberg, E., Wessel, D.: Accelerating Non-Negative Matrix Factorization for Audio Source Separation on Multi-Core and Many-Core Architectures. In: ISMIR. pp. 501–506 (2009)
- [10] Bhattarai, M., Chennupati, G., Skau, E., Vangara, R., Djidjev, H., Alexandrov, B.S.: Distributed non-negative tensor train decomposition. In: 2020 IEEE High Performance Extreme Computing Conference (HPEC). pp. 1–10. IEEE (2020)
- [11] Bhattarai, M., Nebgen, B., Skau, E., Eren, M., et al.: pyDNMFk: Python Distributed Non Negative Matrix Factorization (2021)
- [12] Chennupati, G., Vangara, R., Skau, E., Djidjev, H., Alexandrov, B.: Distributed non-negative matrix factorization with determination of the number of latent features. The Journal of Supercomputing pp. 1–31 (2020)
- [13] Cichocki, A., Zdunek, R., Phan, A.H., Amari, S.i.: Nonnegative matrix and tensor factorizations: applications to exploratory multi-way data analysis and blind source separation. John Wiley & Sons (2009)
- [14] Eswar, S., Hayashi, K., Ballard, G., Kannan, R., Matheson, M.A., Park, H.: PLANC: Parallel Low-rank Approximation with Non-negativity Constraints. ACM Transactions on Mathematical Software (TOMS) **47**(3), 1–37 (2021)
- [15] Everett, B.: An introduction to latent variable models. Springer Science & Business Media (2013)
- [16] Fairbanks, J.P., Kannan, R., Park, H., Bader, D.A.: Behavioral clusters in dynamic graphs. Parallel Computing **47**, 38–50 (2015)
- [17] Févotte, C., Cemgil, A.T.: Nonnegative matrix factorizations as probabilistic inference in composite models. In: 2009 17th European Signal Processing Conference. pp. 1913–1917. IEEE (2009)
- [18] Kannan, R., Ballard, G., Park, H.: A high-performance parallel algorithm for nonnegative matrix factorization. ACM SIGPLAN Notices **51**(8), 1–11 (2016)
- [19] Kim, J., He, Y., Park, H.: Algorithms for nonnegative matrix and tensor factorizations: A unified view based on block coordinate descent framework. Journal of Global Optimization **58**(2), 285–319 (2014)
- [20] Kim, J., Park, H.: Fast nonnegative tensor factorization with an

active-set-like method. In: High-Performance Scientific Computing, pp. 311–326. Springer (2012)

- [21] Koitka, S., Friedrich, C.M.: nmfgpu4R: GPU-Accelerated Computation of the Non-Negative Matrix Factorization (NMF) Using CUDA Capable Hardware. R J. 8(2), 382 (2016)
- [22] Lee, D.D., Seung, H.S.: Learning the parts of objects by non-negative matrix factorization. Nature 401(6755), 788–791 (1999)
- [23] Lopes, N., Ribeiro, B.: Non-negative matrix factorization implementation using graphic processing units. In: International Conference on Intelligent Data Engineering and Automated Learning, pp. 275–283. Springer (2010)
- [24] Mejía-Roa, E., Tabas-Madrid, D., Setoain, J., García, C., Tirado, F., Pascual-Montano, A.: NMF-mGPU: non-negative matrix factorization on multi-GPU systems. BMC bioinformatics 16(1), 1–12 (2015)
- [25] Moon, G.E., Ellis, J.A., Sukumaran-Rajam, A., Parthasarathy, S., Sadayappan, P.: ALO-NMF: Accelerated locality-optimized non-negative matrix factorization. In: Proceedings of the 26th ACM SIGKDD International Conference on Knowledge Discovery & Data Mining, pp. 1758–1767 (2020)
- [26] Phan, A.H., Cichocki, A.: Multi-way nonnegative tensor factorization using fast hierarchical alternating least squares algorithm (HALS). In: Proc. of The 2008 International Symposium on Non-linear Theory and its Applications (2008)
- [27] Phipps, E.T., Kolda, T.G.: Software for sparse tensor decomposition on emerging computing architectures. SIAM Journal on Scientific Computing 41(3), C269–C290 (2019)
- [28] Rabani, E., Toledo, S.: Out-of-Core SVD and QR Decompositions. In: PPSC (2001)
- [29] Sergeev, A., Del Balso, M.: Horovod: fast and easy distributed deep learning in TensorFlow. arXiv preprint arXiv:1802.05799 (2018)
- [30] Tang, B., Kang, L., Zhang, L., Guo, F., He, H.: Collaborative Filtering Recommendation Using Nonnegative Matrix Factorization in GPU-Accelerated Spark Platform. Scientific Programming 2021 (2021)
- [31] Wang, H., Wu, Q., Shi, L., Yu, Y., Ahuja, N.: Out-of-core tensor approximation of multi-dimensional matrices of visual data. ACM Transactions on Graphics (TOG) 24(3), 527–535 (2005)



Ismael Boureima received the B.S. degree in Mechanical Engineering from the University of District of Columbia, Washington, D.C., and the Ph.D. degrees in Mechanical Engineering from the University of North Carolina at Charlotte, NC, USA. His research expertise includes Physics informed machine learning, distributed heterogeneous computing system and computational fluid dynamics. Ismael is a scientist in the Theoretical division as Los Alamos National Laboratory.

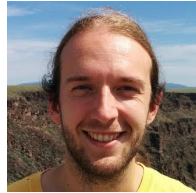


Manish Bhattarai received the M.S. and the Ph.D. degree from the Department of Electrical and Computer Engineering at The University of New Mexico. He is currently a Postdoc Research Associate in the Theoretical division at the Los Alamos National Laboratory in Los Alamos, NM. At LANL, Dr. Bhattarai is part of the tensor factorizations group which specializes on large scale data factorization and improving the Lab's high-performance processing and computing abilities. He has extensively worked on developing HPC

empowered ML algorithms for mining big data such as distributed Matrix and Tensor factorization. His current research interests include: machine learning, computer vision, deep learning, tensor factorizations and high performance computing.



Maksim E. Eren is a graduate Computer Science student at the University of Maryland Baltimore County (UMBC) and a Scholarship for Service CyberCorps alumnus. He graduated Summa Cum Laude with a Computer Science Bachelors at UMBC in 2020. He has held multiple internships, which have ranged from incident response and software engineering at Montgomery County Government (MCGov), a research assistantship at CyberPacks, to a teaching assistantship at UMBC. Currently, he is working as a graduate research assistant at Los Alamos National Laboratory (LANL) and at UMBC's DREAM Lab. His interdisciplinary research interests lie at the intersection of machine learning and cybersecurity, with a concentration in tensor decomposition.



Erik Skau received the B.Sc. degree in applied mathematics and physics, and the M.Sc. and Ph.D. degrees in applied mathematics from North Carolina State University, Raleigh, NC, USA. His research expertise includes optimization techniques for matrix and tensor decompositions. Erik is a scientist in the Information Sciences Group as Los Alamos National Laboratory.



Philip Romero received the M.S. degree in mechanical engineering and the M.B.A. degree from Stanford University. He is a Computer Scientist with the High-Performance Computing Environments Group (HPC-ENV), Los Alamos National Laboratory. His research interests include machine learning, deep learning, data science and visualization, quantum computing, and performance modeling and simulation.



Stephan Eidenbenz received the Ph.D. degree in computer science from the Swiss Federal Institute of Technology, Zurich (ETHZ). He is a Computer Scientist with the Information Sciences Group (CCS-3), Los Alamos National Laboratory (LANL). Prior to that, he was the Director of the Information Science and Technology (ISTI) Institute, LANL. His research interests include cybersecurity, computational co-design, communication networks, scalable modeling and simulation, and theoretical computer science



Boian Alexandrov is a senior scientist at the Theoretical Division in Los Alamos National Laboratory. He has MS in Theoretical Physics, a PhD in Nuclear Engineering and second PhD in Computational Biophysics. Alexandrov is specialized in Big Data analytics, non-negative Matrix and Tensor Factorization, Unsupervised Learning, and Latent Feature Extraction.